Improved Pole Placement and Compaction of MIMO Vector Fitting Applied to System Identification

Andrew Macmillan Smith, *Member, IEEE,* Salvatore D'Arco, Jon Are Suul, *Member, IEEE,* and Bjørn Gustavsen, *Fellow, IEEE*

***Abstract*—In this work we address the modeling of multi-port subsystems with unknown inner dynamics by utilizing vector fitting to identify state-space models for performing eigenvalue-based analysis. Vector fitting is used to characterize frequency responses obtained from frequency domain analysis, for example, from Fourier transformation of time domain data. The intended use is for interconnection with other models in system stability analysis, where the use of compact state-space models is desirable. Typically, vector fitting of a multiple-input/multiple-output (MIMO) system leads to a large state-space model where each column (input) is fitted by a common pole set using a predefined model order. An alternative vector fitting process based on a pole collapsing scheme is proposed which can find suitable poles for a more compact state-space model. Additionally, a method for simpler, more automated order determination is introduced. The use of the presented approach for obtaining a fully compacted model (without pole repetitions) is examined and compared against a previously proposed method based on singular value decomposition. Application to an example system representing a 2-level power electronic converter demonstrates that the proposed method gives a model with improved accuracy of eigenvalue identification and model compaction, while retaining the essential information in terms of system dynamic behavior.**

***Index Terms*—vector fitting, MIMO system, black-box modeling, pole location, order selection, compaction**

NOMENCLATURE

$\mathbf{FC_{HSV}}$	Full compaction based on balanced truncation.
HSV	Hankel singular value.
MF	Matrix fitting.
MIMO	Multiple-input/multiple-output.
PC-CF	Pole-collapsing column fitting.
SAE	Sum of absolute errors.
SVD	Singular value decomposition.
VF	Vector fitting.

Manuscript received August 11, 2023; revised December 1, 2023; accepted January 20, 2024. Date of publication February xx, 2023; date of current version February 8, 2024. Paper no. TPWRD-01128-2023. This work was supported by the Ocean Grid Research Project, funded by the Green Platform instrument of the Research Council of Norway under Grant 328750. (Corresponding author: Andrew Macmillan Smith.)

Andrew Macmillan Smith, Salvatore D'Arco and Bjørn Gustavsen are with SINTEF Energy Research, 7465 Trondheim, Norway (e-mail: Andrew.Smith@sintef.no, salvatore.darco@sintef.no, bjorn.gustavsen@sintef.no)

Jon Are Suul is with SINTEF Energy Research, 7465 Trondheim, Norway, and also with the Department of Engineering Cybernetics, Norwegian University of Science and Technology, 7491 Trondheim, Norway (e-mail: Jon.A.Suul@sintef.no

Color versions of one or more of the figures in this paper are available online at http://ieeexplore.ieee.org.

Digital Object Identifier 10.1109/TPWRD.2014.xxxx

I. INTRODUCTION

STATE-space models offer several advantages for analysing the behaviour of dynamic systems and form the basis for large parts of modern control theory [1]. Access to a state-space model also provides significant flexibility in the available tools for analyses and the type of simulations that can be performed. In particular, the stability of a linear system can be easily determined from the state-space model by examining the eigenvalues [2]. Additionally, nonlinear systems can be linearized around an operating point and provide similar analyses for small-signal dynamics [2]. To formulate a state-space model with an analytical approach requires detailed, comprehensive information about the studied system and its parameters. Additionally, the required information is usually not available for commercial products due to confidentiality requirements. Instead, black-box models for time-domain simulation are commonly utilized to represent such systems, where the internal details are not revealed and only access to external ports is available. However, techniques have been developed to create mathematical models using only input and output signals. Such system identification methods can provide a state-space model from a black-box model [3]. Although originally developed as a fitting tool, vector fitting (VF) can be used as a system identification tool.

VF was introduced by Gustavsen and Semlyen in 1999 [4] and has since received much attention due to its open-source code, ease of use, and wide suitability. Thus, the reported range of applications for VF is broad and varied, from simulation of transmission line transients [5] and thermal modeling of batteries [6] to controller parameter estimation [7] or incorporation into transfer function estimation in Matlab [8]. Furthermore, many publications have suggested improvements and modifications to the original method. Some of these improvements have been incorporated into the open-source code provided at the vector fitting website, such as "relaxed vector fitting" for removal of biasing [9], and a fast implementation reducing the computation time of the algorithm [10].

In general, the VF algorithm provides a pole-residue model from the frequency response curves of a system, which can be easily converted to a state-space model. VF was originally designed for single-input/single-output or single-input/multiple-output systems, but the extended *column fitting (CF)* and *matrix fitting (MF)* [11] algorithms were developed for use with MIMO systems. The design-case for these adaptations

of VF was primarily for admittance matrices; however, the use cases have extended beyond. The matrix fitting website provides several examples of use cases [12].

Furthermore, the matrix fitting algorithm can identify a common set of poles for all the inputs, in contrast to column fitting which fits a common pole set to each column. A real system has a common set of poles that are based on physical and control parameters of the system, and so the common pole set produced by matrix fitting is more representative of a real system. Although the columns (inputs) share a common pole set, matrix fitting will produce a state-space system with these poles repeated for each column [13]. This can lead to much larger state-space models than would be determined analytically, and therefore more computationally expensive models. Additionally, a model with repeated poles is less representative of the real system, which is significantly more constrained in number of variables. A method of compacting the state-space model to have fewer or no repeated poles was therefore presented in [13] at the cost of increased error in the model.

Regardless of the number of inputs/outputs, VF requires the user to select an order. The conventional method is based on "trial and error" by successively increasing/decreasing the order to optimize the trade-off between a low order and sufficiently small error for the application. Such a method requires iteration from the user and order selection is not always straightforward. For example, frequency response data with some random deviations and noise will be fitted more accurately with progressively higher order; however, the noise will also be fitted, leading to over-fitting and a deceptively high order selection.

This work attempts to address these issues and extends the functionality of vector fitting with respect to system identification of MIMO systems. The two main contributions of this work can be summarized as:

1) A novel method for determining poles for vector fitting is proposed, named pole-collapsing column fitting (PC-CF). This method is characterized by:
   - Increased pole placement accuracy compared to matrix fitting.
   - Appropriate order selection, less prone to overfitting.
2) Introduction of a compaction method with reduced model error.

The paper is organized as follows. First, the VF algorithm is briefly described to give proper context for the introduction of the new method. Then, the new MIMO system vector fitting method is presented with a simple example to highlight the difference in comparison to matrix fitting and demonstrate its use. Subsequently, the theoretical basis for system compaction is presented, including changes to previously proposed methods. The methods are demonstrated on a more detailed, realistic example system (a power electronics converter), and finally the main results from this work are discussed and summarized.

II. Classical Vector Fitting

This section examines the basic vector fitting algorithm and its application process to provide context.

A. Vector Fitting Algorithm

VF approximates a given scalar or vector frequency response $\mathbf{f}(s)$ with a pole-residue model (1), defined by *N* poles, p_n, and residues, $\mathbf{c}_n$, where terms $\mathbf{d}$ and $\mathbf{e}$ can be zero [4].

$$\mathbf{f}(s) = \sum_{n=1}^{N} \frac{\mathbf{c}_n}{s - p_n} + \mathbf{d} + s\mathbf{e} \tag{1}$$

VF iteratively relocates the initial poles using a linear least-squares approach, and then calculates the residues. The system order and placement of poles are determined as follows.

1) Order Selection: The number of poles, or the order, is usually selected by a "trial and error" method, progressively increasing the order until the responses are fitted with sufficient accuracy. Although some reasonable guesses can be made for the order based on the observed frequency response, this still results in an iterative solution that requires input from the user, and may capture only the most apparent poles. In the case where a system is linearized around an operating point, the influence of a pole may change at each operating point and give different apparent orders. If many operating points are examined, this may become cumbersome.

2) Pole Location: It is important to note that vector fitting first iteratively relocates the poles before calculating the final residues for each pole. When using matrix fitting for a MIMO system, the frequency responses for each column (inputs in a MIMO system) are combined into a single column [11]. This single column is fitted with one set of poles, and the residues can then be calculated for each input. In this way, the MIMO system is vector fitted with a common pole set. Note that matrix fitting was originally developed for square admittance matrices where reciprocity must be preserved, so some minor adjustments must be made to adapt the open-source code for non-square MIMO systems.

B. Conversion from Pole-Residue Model to State-Space Model

1) SISO and SIMO Systems: Once a pole-residue model is obtained, it is a straightforward process to convert to a state-space model. For a general system with one input, a total of *J* outputs, and *N* poles, the $\mathbf{A}$ matrix will be an $N \times N$ diagonal matrix, with each pole, p_n, placed on the diagonal. The $\mathbf{B}$ matrix is simply a $N \times 1$ ones matrix, while the $\mathbf{C}$ matrix places the residues for each pole, c_n, into a column, creating a $J \times N$ matrix. The $\mathbf{D}$ matrix is a $J \times 1$ matrix, with the feedthrough values for each output, d_j, in the column vector. The following demonstrates how the matrices are constructed.

$$\mathbf{A} = \begin{bmatrix} p_1 & 0 & \dots & 0 \\ 0 & p_2 & \dots & 0 \\ \vdots & \vdots & \ddots & \vdots \\ 0 & 0 & \dots & p_N \end{bmatrix}, \quad \mathbf{b}^T = \begin{bmatrix} 1 & 1 & \dots & 1 \end{bmatrix} \tag{2}$$

$$\mathbf{C} = \begin{bmatrix} c_{1,1} & c_{1,2} & \dots & c_{1,N} \\ c_{2,1} & c_{2,2} & \dots & c_{2,N} \\ \vdots & \vdots & \ddots & \vdots \\ c_{J,1} & c_{J,2} & \dots & c_{J,N} \end{bmatrix}, \quad \mathbf{d}^T = \begin{bmatrix} d_1 & d_2 & \dots & d_J \end{bmatrix} \tag{3}$$

2) MIMO Systems: Several methods for applying vector fitting to a MIMO system are discussed in [14]. These are defined as single-element fitting (multi-SISO structure), single-column fitting (multi-SIMO structure), and matrix fitting (MIMO structure). The difference between these methods is the degree to which poles are shared, with single-element fitting sharing no common poles, column fitting sharing common poles for each column (as shown in (2) and (3)), and matrix fitting sharing common poles for the entire MIMO system. The methodology of matrix fitting is shown below as it is also relevant to this work.

After fitting a common pole set to the system as described previously, the residues for each input can be assembled into a larger state-space system. For a total I number of inputs, the matrices can be constructed as follows, where $\mathbf{A_c}$ is the matrix with common poles, $\mathbf{b_i}$ is the column vector for input i, $\mathbf{C_i}$ is the $\mathbf{C}$ matrix for input i, and $\mathbf{d_i}$ is the column vector for input i, all constructed according to (2) and (3). Note that $\mathbf{A_c}$ is repeated I times.

$$\mathbf{A} = \begin{bmatrix} \mathbf{A}_\mathrm{c} & 0 & \dots & 0 \\ 0 & \mathbf{A}_\mathrm{c} & \dots & 0 \\ \vdots & \vdots & \ddots & \vdots \\ 0 & 0 & \dots & \mathbf{A}_\mathrm{c} \end{bmatrix}, \mathbf{B} = \begin{bmatrix} \mathbf{b}_1 & 0 & \dots & 0 \\ 0 & \mathbf{b}_2 & \dots & 0 \\ \vdots & \vdots & \ddots & \vdots \\ 0 & 0 & \dots & \mathbf{b}_\mathrm{I} \end{bmatrix} \quad (4)$$

$$\mathbf{C} = \begin{bmatrix} \mathbf{C}_1 & \mathbf{C}_2 & \dots & \mathbf{C}_\mathrm{I} \end{bmatrix}, \mathbf{D} = \begin{bmatrix} \mathbf{d}_1 & \mathbf{d}_2 & \dots & \mathbf{d}_\mathrm{I} \end{bmatrix} \quad (5)$$

Constructing the matrices in this way gives a state-space matrix that contains significantly more states than the physical system. Whether such a large state-space system is acceptable is debatable and may depend on the application. This expanded form allows more degrees of freedom for vector fitting, which as demonstrated later, can result in a more accurate system model. However, the system will result in more computationally expensive simulations. A fully-compacted state-space system (without repeated poles but with a full B matrix) is approximately $I/2$ times more efficient in time-domain simulations, depending on the solver [13]. For this reason, among others, an attempt to compact the state-space model is made in this work.

3) Complex-Valued to Real-Valued State-Space: The methods for creating the state-space matrices described thus far use complex-valued matrices, i.e. the poles on the diagonal of $\mathbf{A}$ can be complex. This can cause problems when using simulation software, as state-space matrices are often required to be real-valued only. Therefore, real-valued realizations are assumed in this work unless otherwise stated. The above state-space matrices can be converted to real-only valued matrices according to [4]. For an imaginary pole pair, $p = p' \pm jp''$, the sub-matrices for the two poles are then altered to:

$$\mathbf{A_p} = \begin{bmatrix} p' & p'' \\ -p'' & p' \end{bmatrix}, \quad \mathbf{b_p} = \begin{bmatrix} 2 \\ 0 \end{bmatrix} \quad (6)$$

$$\mathbf{C_p} = \begin{bmatrix} real(c) & imag(c) \end{bmatrix} \quad (7)$$

III. Pole-Collapsing Column Fitting

This section presents a novel method of VF for a MIMO system, called PC-CF. This method can be loosely described as a combination of column fitting (multi-SIMO structure) and matrix fitting (MIMO structure). A pole set is fitted to each column (in this case equivalent to the outputs for an individual input) and then "collapsed" into a single common pole set for the MIMO system, after which the residues are calculated. This method is characterized by increased accuracy in pole placement and simplified order selection compared to matrix fitting, while still using a common pole set for the system.

The selection of model order is not a trivial problem, and many other system identification or fitting methods also require an explicit selection of the model order (e.g. N4SID [15]). Aside from the trial and error method commonly used with VF, another approach is to use the Hankel singular values (HSVs) to recommend an order. The Hankel singular values, σ_H, are defined as the square root of the eigenvalues of the product of the controllability grammian, $\mathbf{W}_C$, and the observability grammian, $\mathbf{W}_O$ (8), where the controllability and observability grammians are the solutions to the following two Lyapunov equations (9), (10), respectively. These equations can be solved using well-known and scalable methods.

$$\sigma_H = \sqrt{\mathrm{eig}(\mathbf{W_C W_O})} \quad (8)$$

$$\mathbf{A W_C} + \mathbf{W_C} \mathbf{A}^T = -\mathbf{B B}^T \quad (9)$$

$$\mathbf{A}^T \mathbf{W_O} + \mathbf{W_O A} = -\mathbf{C}^T \mathbf{C} \quad (10)$$

The HSV approach uses singular value decomposition of the Hankel matrix, which gives an indication of each state's importance. Typically, the HSVs are plotted and significant drops in value between two states indicate that the rest can be discarded, which gives the indication of a suitable model order. Although this method can provide a good determination of order, it is not always reliable. A simple example can demonstrate this. A system of order four is defined as follows:

$$\mathbf{A} = \begin{bmatrix} -0.2 & 0.4 & 0 & 0 \\ -0.4 & -0.2 & 0 & 0 \\ 0 & 0 & -0.4 & 0.2 \\ 0 & 0 & -0.2 & -0.4 \end{bmatrix}, \mathbf{B} = \begin{bmatrix} 1 & 2 \\ 1 & 2 \\ 1 & 2 \\ 1 & 2 \end{bmatrix} \quad (11)$$

$$\mathbf{C_1} = \begin{bmatrix} 100 & 100 & 100 & 100 \end{bmatrix} \quad (12)$$

$$\mathbf{C_2} = \begin{bmatrix} 100 & 100 & 2 & 2 \end{bmatrix} \quad (13)$$

Note that two alternative $\mathbf{C}$ matrices are used to highlight the difference this creates in the HSV evaluation. A plot of the frequency response of the system is given in Fig. 1. The data input used for VF are frequency responses constructed with 800 samples logarithmically spaced from 10^{-2} to 10^2 Hz.

Fig. 2a shows that when using $\mathbf{C}_1$ to generate the HSVs from the frequency response data, the HSVs give a good indication of model order. There is a significant drop after order four, which provides evidence for selecting this order.

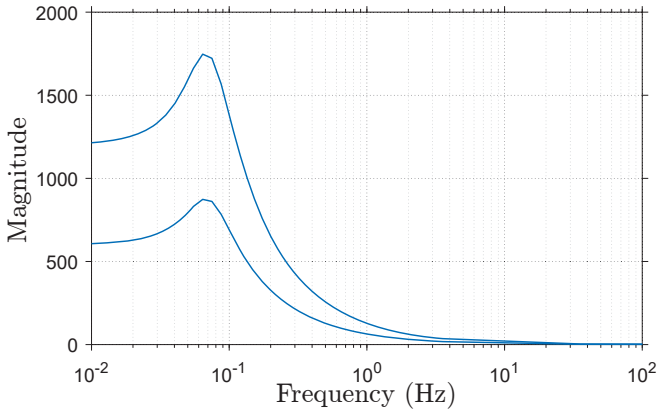

Fig. 1. Frequency response of example system, using $\mathbf{C_1}$

.

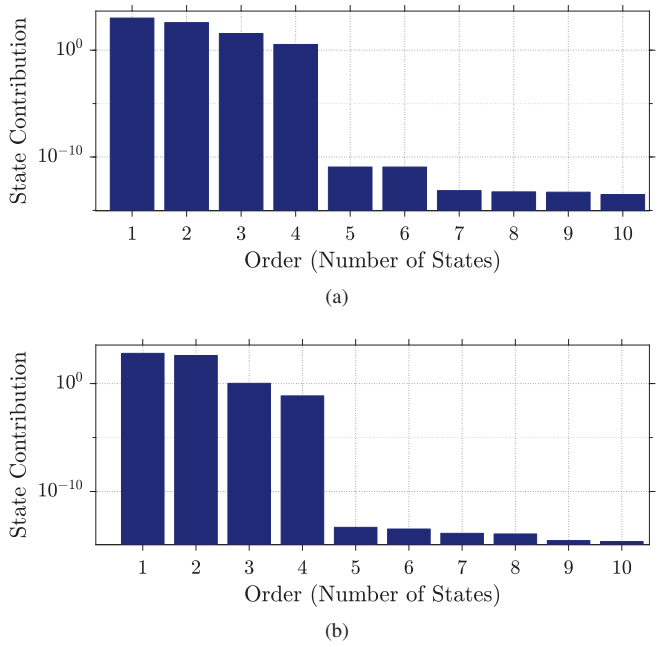

Fig. 2. Hankel singular values comparing sample system with different $\mathbf{C}$ matrices. (a) Values using $\mathbf{C_1}$. (b) Values using $\mathbf{C_2}$.

However, when using frequency responses derived from the system using $\mathbf{C}_2$, the HSVs do not provide such a clear indication of order. Fig. 2b shows a drop after order two and another drop after order four, and so determination of the order is ambiguous. This can be even more inconclusive for a system with more poles and without any clear drops in value. It can be argued that states with low HSVs can be safely ignored, but without knowledge of the system, it can be difficult to make a decision on where an acceptable cut-off is. This is more apparent in the example in Section V.

To determine the correct order, and to more accurately locate the poles, a novel method is presented. In contrast to matrix fitting, which fits a common set of poles to all the data columns, an initial pole set is fitted to each input separately, as in column fitting. The first column (input) responses are fitted iteratively to find the poles for that column. Each successive

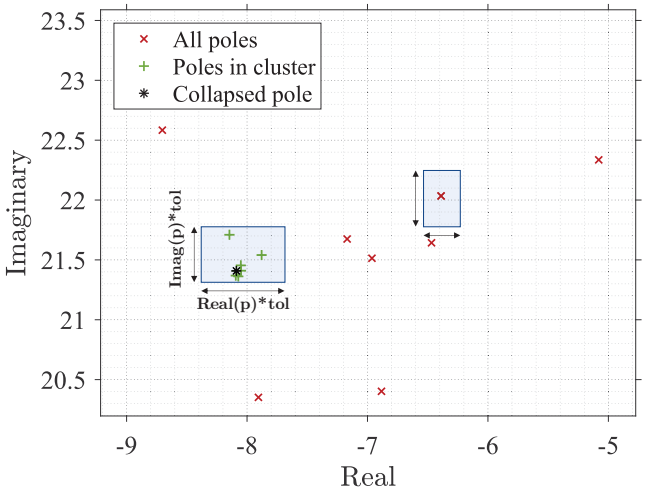

Fig. 3. Example of pole collapsing from a large initial pole set.

column is then fitted separately. Eq. (1) can be rewritten in column fitting form for each column i as:

$$\mathbf{f}_i(s) = \sum_{n=1}^{N} \frac{\mathbf{c}_{i,n}}{s - \mathbf{p}_{i,n}} + \mathbf{d}_i + s\mathbf{e}_i \quad , i = 1, 2, ..., I \qquad (14)$$

The total initial pole set can then be given as the union of all column pole sets:

$$P_{initial} = \bigcup_{i=1}^{I} \bigcup_{n=1}^{N} p_{i,n} \qquad (15)$$

When a relatively high number of poles are used for each column in this successive fitting (i.e. N in (14) is two to three times the expected order of the system), the "true" poles become convergent and the rest are largely random or fitted to noise in the data. Thus, the "true" poles of the system can be discovered by examining the poles which are common between each column. The poles that are overlapping (with some small tolerance) between several inputs can be chosen as the common poles of the system.

Fig. 3 demonstrates how the poles are collapsed. Note that the Sec. V system is used to better highlight the methodology. The tolerance used is taken as a percentage of the real and imaginary components of each pole. This will result in a tolerance area that scales by proximity to the origin. This allows for lower frequency oscillations (associated with poles nearer the origin) to be fit with similar relative accuracy as higher frequency oscillations. If there are at least two other poles within this tolerance rectangular area (one other pole if there are only two inputs in the system), this pole is treated as a cluster. The figure shows how this tolerance area changes depending on the location of the pole in the complex plane. Then the pole nearest to the median of this cluster of poles is taken to be the singular collapsed pole for that cluster.

The selection of the tolerance is important and affects how many common poles are found but this tolerance is much

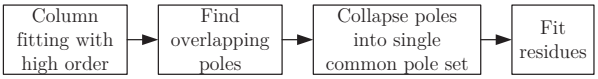

Fig. 4. PC-CF process diagram.

less sensitive than selecting the order manually. Furthermore, the tolerance more directly relates to the noise and error in the measured frequency responses. Frequency responses with higher noise need a larger tolerance as the poles will not converge as precisely as with a data set with low noise. In the sample system used in Section V, 3% is used, and generally a tolerance of 1-10% is suggested. The overall poles of the system are determined by selecting only those overlapping poles, and the number of these poles gives an approximate order of the system. This collapsing process is reminiscent of a stabilization diagram [16]. A stabilization diagram can indicate the true modes of a system by examining which modes are consistent when identifying at different model orders, where those repeating over a wide range of orders can be taken as true poles, while those appearing inconsistently can be treated as purely mathematical poles. Instead of stability over model order, PC-CF can be said to examine stability between inputs. Reference [16] suggests using a 1-5% tolerance for determining mode stability. Additionally, several mode-clustering methods for stabilization diagrams are examined in [17], providing further basis for collapsing multiple close poles into one.

The poles found in the pole-collapsing method can then be used as the common pole set to find the residues in a standard vector fitting manner. Fig. 4 describes the total PC-CF process. The common pole set between all columns, as opposed to unique pole sets for each column, allows for further model compaction, discussed in the next section.

When PC-CF is applied to the state-space system given by (11) and (13) ($\mathbf{C}_2$), the order found is four. This system has an ambiguous order selection based on HSVs. If the $\mathbf{C}$ matrix is altered such that the third and fourth states have an HSV as low as the subsequent states (i.e. 10^{-12}), this would give a clear indication for order two according to HSV analysis. However, PC-CF is still able to find all four poles.

To demonstrate the improved pole finding ability of PC-CF compared to matrix fitting, the system is examined using both $\mathbf{C}_1$ and $\mathbf{C}_2$. The difference can be highlighted best when the number of poles found is less than the actual system order, i.e. underfitted. Therefore, the pole overlapping tolerance (shown in Fig. 3) is set to an extremely low value, 10^{-12}. With this tolerance, PC-CF finds only one pole pair. Matrix fitting is also used with an order of two.

Fig. 5 shows that PC-CF locates the two poles closer to the theoretical poles than MF, especially when $\mathbf{C}_1$ is used. This is because MF attempts to fit all four poles to a reduced set of two poles. This effectively "drags" one pole pair towards the 2nd pole pair to compensate. As the relative contribution of the 2nd pole pair increases (from $\mathbf{C}_2$ to $\mathbf{C}_1$), this behavior becomes more pronounced and the poles are dragged further.

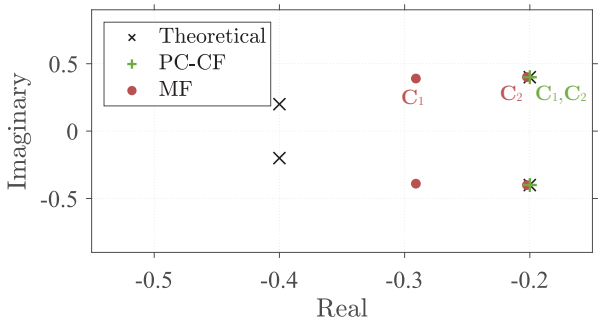

Fig. 5. Pole location, PC-CF vs matrix fitting.

PC-CF places the poles first with higher order, and so is not affected in the same way, resulting in more accurate placement of these two poles.

It is also possible to fit the model with MF by using a high initial order and then reduce the model to the poles with the highest HSV. This will give a similar pole placement to PC-CF in this simple case but it can result in undesirable behavior in more complex systems. This is addressed further in Section V. Note that in a case such as this, the increased accuracy of the poles will typically come at the cost of increased error in the frequency response. The consequences of the difference in pole placement are discussed further in Section VI.

Although the system is demonstrated with a very simple example, the process can be expanded to higher orders and more complex systems. In fact, the difficulties with order selection and accurate pole location are typically more pronounced in more complex systems, as is demonstrated in Section V.

IV. Model Compaction

Obtaining a state-space model with as few repeated poles as possible can increase the computational performance, especially when combining multiple systems together. Therefore, two alternative state-space model compaction methods of vector-fitted systems are examined, specifically a method based on singular value decomposition (SVD) and a method based on balanced truncation.

A. Compaction Using Singular Value Decomposition (SVD)

The compaction process described in [13] is used as a framework for this section. SVD is performed on the residue matrices (in complex form) for each pole, where the residue matrix for a single pole, $\mathbf{R_p}$ can be written as the multiplication of three matrices:

$$\mathbf{R_p} = \mathbf{U}\boldsymbol{\Sigma}\mathbf{V}^T \tag{16}$$

Here $\boldsymbol{\Sigma}$ is a matrix containing the singular values, σ, on the diagonal in descending order. It should be noted that the number of non-zero singular values is equal to the rank of $\mathbf{R_p}$. Originally, each pole will be repeated by the number of columns (inputs), I. The number of repeated poles kept during compaction can be determined by the number of singular values kept. With an r number of retained singular values,

the $\mathbf{B}$ and $\mathbf{C}$ matrices for a specific pole, $\mathbf{B_p}$ and $\mathbf{C_p}$, are found by:

$$\mathbf{B_p} = \mathbf{V}^T(1:r,:) \tag{17}$$

$$\mathbf{C_p} = \mathbf{U}(:,1:r)\mathbf{\Sigma}(1:r,1:r) \tag{18}$$

The result is that the rank of the residue matrix is reduced to the number of singular values retained. The compaction performed on the full state-space system can be performed according to various degrees. As discussed in [13], the number of retained singular values of the residue matrices can be defined by a threshold, ρ, between the first and the last retained singular values:

$$\frac{\sigma_r}{\sigma_1} < \rho \tag{19}$$

The minimal realization for a system (where the state-space system is both controllable and observable) is the number of common poles times the number of ports [14]. Although correct, this lacks completeness when dealing with a system which is explicitly input-output instead of a port representation, and therefore may be non-square. For a residue matrix of a single pole, $\mathbf{R_p}$, with *I* inputs and *J* outputs, $\mathbf{\Sigma}$ will be an $I \times J$ matrix. As the rank is given by the number of singular values on the diagonal, the rank will be determined by:

$$\text{rank}(\mathbf{\Sigma}) = \text{rank}(\mathbf{R_p}) = \min(I, J) \tag{20}$$

Therefore, the minimal realization for a MIMO system with *n* common poles will be order $\min(I, J) \cdot n$. With a square system, this is equivalent to that in [14]; however, for a system with $J < I$, this implies the order of the minimal realization will be governed by *J*, and not *I*. The pole repetitions can then be reduced to *J* repetitions, without loss of accuracy in the resulting state-space model. This can be achieved in practice by simply setting the compaction threshold to zero, such that all the singular values are retained.

To compact the system such that there are no repeated poles, one singular value can be used for each pole. This can be achieved by setting the compaction threshold in (19) to unity. Note that choosing a threshold between zero and one will result in some repeated poles but fewer than the original system.

B. Compaction using Balanced Truncation

Another way to perform the compaction is to use the Hankel singular values (Eq. 8) of the state-space system defined by a single pole. Order reduction using balanced truncation of the state-space system (given by $\mathbf{A_p}$, $\mathbf{B_p}$, $\mathbf{C_p}$, and $\mathbf{D}$) based on the HSVs results in a similar compaction for each pole as the SVD method. The major difference from Section IV-A is that SVD is used on the product of the controllability and observability grammians instead of directly on the residue matrix. Balanced truncation is a common technique for order reduction of state-space systems and retains the highest "energy" poles, and by using the HSVs, the pole repetitions can be reduced in a way to better retain the behavior of the system [18]. The same threshold criterion as (19) can be used for selecting how many HSVs to retain and thereby the degree of compaction, modified to:

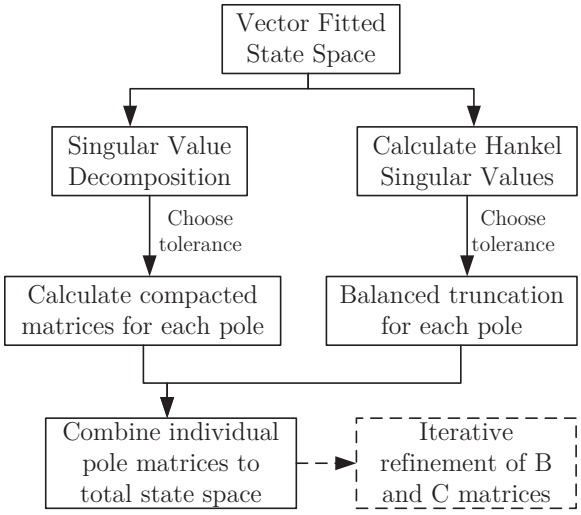

Fig. 6. Compaction flowchart with compaction based on SVD or balanced reduction.

$$\frac{\sigma_{H,r}}{\sigma_{H,1}} < \rho \tag{21}$$

where σ_H are the HSVs found by applying (8). It should be noted that this is performed on the system after it has been converted to real-valued matrices, using the process described in (6) and (7). It is demonstrated later that compacting the system based on balanced truncation is generally more accurate than using the SVD-based method.

C. Iterative Refinement

Compaction will typically result in increased model errors, as some information is lost in the compaction. The work in [13] used an iterative nonlinear solver for improving the resulting compacted system. Therefore, the compacted system is improved in the frequency domain in this work using an iterative refinement process. A nonlinear optimization of $\mathbf{B}$ and $\mathbf{C}$ is performed, while the $\mathbf{A}$ matrix is not altered. In this case, the Matlab function `pem` is used, which uses prediction error method and various solver methods to optimize a system. A unitary weighting scheme is used for the refinement.

Fig. 6 shows a flowchart for the compaction process according to the two methods discussed, with optional iterative refinement. The iterative refinement process is the same regardless of whether the original compaction is done using SVD or balanced truncation.

V. Application Example

This section demonstrates the proposed vector fitting method compared to MF, as well as a comparison of compaction methods. A Simulink model of a 2-level voltage source

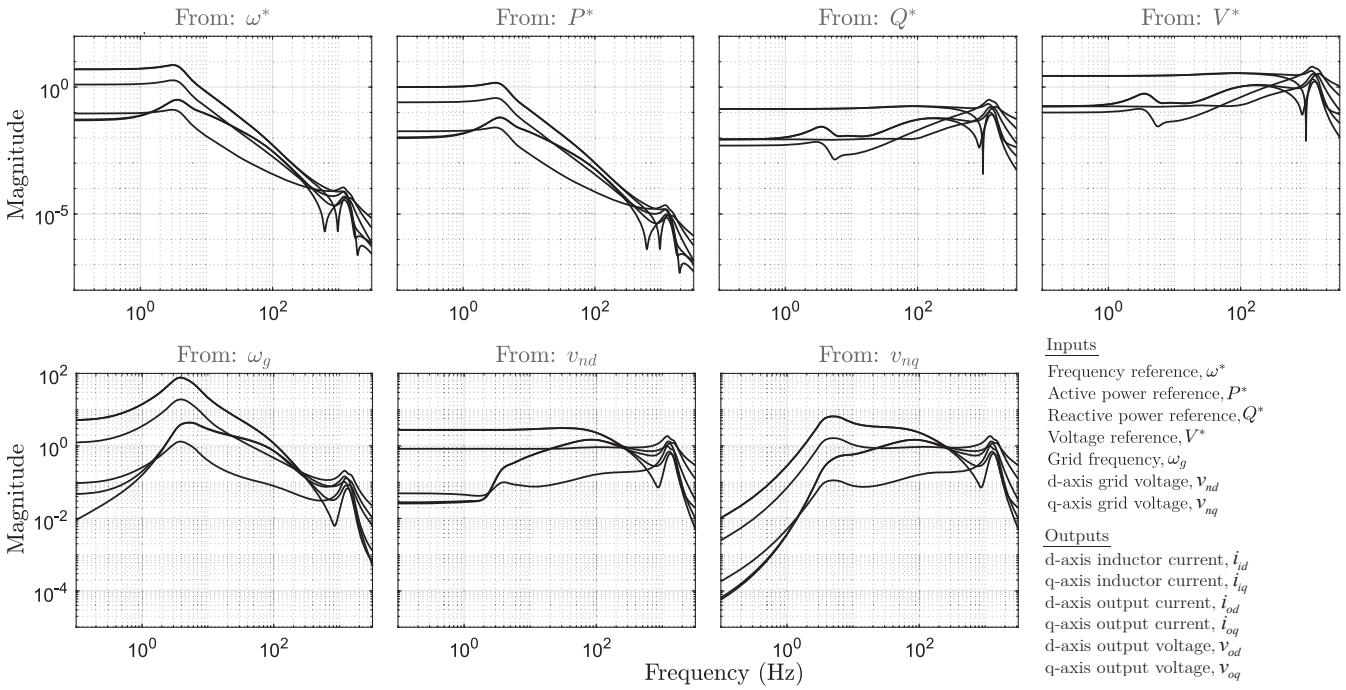

Fig. 7. VSM model frequency responses. Example with I=7 inputs and J=6 outputs, obtained from time-domain simulations.

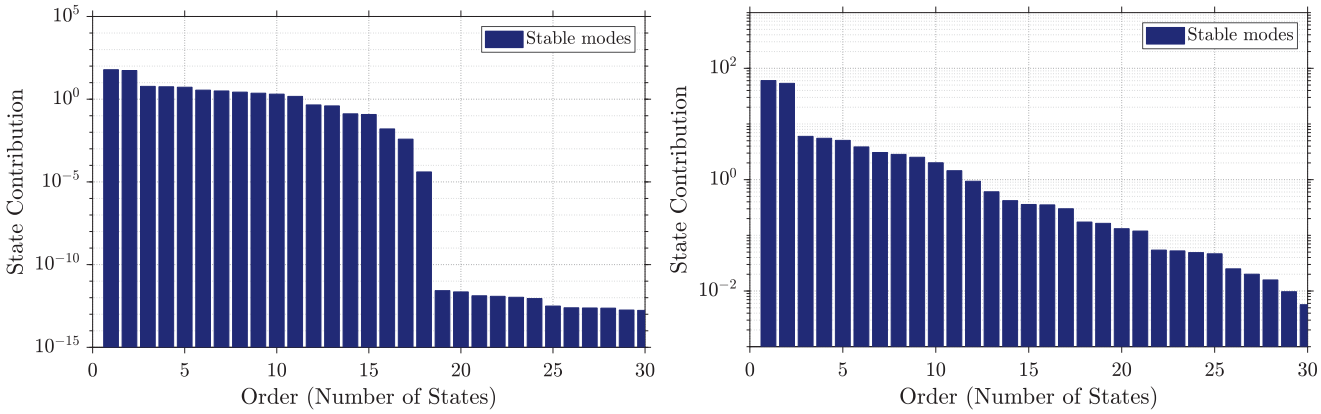

Fig. 8. Hankel singular values for example VSM system. (a) Values using theoretical system. (b) Values using Simulink model.

converter is used to evaluate the accuracy and simulation CPU time according to several metrics. The frequency responses for the system with 7 inputs and 6 outputs are shown in Fig. 7.

The two VF methods with common pole sets (PC-CF and MF) as well as compaction using SVD versus balanced truncation of each method are compared. The same order as found from PC-CF is used for matrix fitting to give a fair comparison. To demonstrate the differences between compaction methods more clearly, the systems are fully compacted such that they have no repeated poles (compaction threshold of one). The **B** and **C** matrices of the compacted systems are improved with the Matlab function `pem` to demonstrate the increased accuracy achieved by refinement.

A. *Example System*

A 2-level converter controlled as a virtual synchronous machine is used as an example, based on the models developed in [19] and [20]. Note that the analytical state-space formulation is available for this model; however, the analytical model is only used to assess the accuracy of pole placement of the resulting identified models. Frequency responses obtained from time-domain simulations of the Simulink model are used for the fitting process, referred to as simulated frequency responses. Specifically, a frequency sweep of single-tone sinusoidal inputs is performed, output responses are measured, and the Fast Fourier Transform (FFT) is performed on the input and output time series to obtain the frequency responses. These simulated responses are used as opposed to the analytical

ones as they represent a more realistic system identification scenario, with noise and errors more typical of frequency responses found from simulated, experimental, or operational data. The analytical counterpart is necessary to determine the accuracy of the identified eigenvalues from the fitted models, which are otherwise unavailable from frequency responses.

It should be noted that the selected system is nonlinear in nature, while VF is able to provide linear identified models. However, linear models can accurately represent the dynamics of a nonlinear system for small perturbations around an operating point, and the resulting frequency responses and state-space models remain valid for small-signal analyses [2]. Therefore, VF or other linear system identification techniques are directly applicable for obtaining small-signal models from the frequency responses of nonlinear systems. The limitation is that the input perturbations during the time-domain simulations or experiments for frequency scanning must be kept sufficiently small to maintain validity of the small-signal approximation, and that the obtained model will only be valid at the studied operating point. This process has also been applied in [7], [21], [22]. For the studied example, the validity of small-signal models has been demonstrated in [19], [20].

The selected model is also suitable for illustrating the difficulty in defining a system order based on the HSVs from simulated frequency responses, as shown in Fig. 8. Moreover, this model represents a MIMO system with an unequal number of inputs and outputs. System identification of power electronics systems presents a technically challenging case, with practical applications [22], [23], [24]. Finally, this model provides an excellent example of how the proposed VF method can be used to increase the accuracy of VF of a MIMO system for eigenvalue identification and analysis.

The inputs and outputs are listed in Fig. 7. The number of inputs, *I*, is 7, and the number of outputs, *J*, is 6. By using the control references as inputs, the entire system including the physical system components and the control system are included in the resulting identified system model. Note that the simulated system frequency responses are used for fitting, not those from the analytical system model.

B. Evaluation of Accuracy and Efficiency

The classic MF, PC-CF, and the compacted models of each are examined for their ability to fit the test system from a set of frequency responses.

1) Eigenvalues: PC-CF and matrix fitting are examined for their ability to find the correct eigenvalues of the system. It should be noted that the eigenvalues are not of equal importance in an eigenvalue analysis. The Hankel singular values (HSVs) effectively describe the magnitude of each state's importance on the input/output behavior [25]. In canonical form, a state can then be directly correlated with an eigenvalue of the system. Eigenvalues with a small HSV will have little effect on the system, and therefore are of relatively low importance.

For each eigenvalue in the known analytical system model, p_n, the distance in the complex plane, d_n, to the closest eigenvalue in the identified model is found and normalized by the distance to the origin. A weighted sum of these errors gives an overall measure of the error in the eigenvalue location accuracy. This fitting accuracy can be found by:

$$\text{rel error} = \sum_{n=1}^{N} w_n \cdot \frac{|d_n|}{|p_n|} \tag{22}$$

where w_n is the weighting for an eigenvalue. A weighting scheme based on the HSVs is given as:

$$w_n = \frac{\sigma_{H,n}}{\max(\sigma_H)} \tag{23}$$

where $\sigma_{H,n}$ is the HSV for an eigenvalue. Therefore, the eigenvalues are given weights according to magnitude of the corresponding HSVs. Unitary weighting is also applied to (22) to give equal weight to all eigenvalues.

Fig. 9 shows a comparison of eigenvalues found from the proposed PC-CF as opposed to MF. PC-CF is used with an initial pole count of 50, and MF is used with the same order as found by PC-CF, such that the final pole count is equivalent. PC-CF finds a total of 14 poles for the system, out of 19 in the theoretical state-space. As seen in Figure 9 at approximately -100 on the real axis, three of these poles are located quite closely together, and PC-CF finds one pole for these three combined. Additionally, from Fig. 8a, only 17 or 18 poles are actually relevant. Therefore, an order of 14 is reasonable. If the frequency responses are generated from the analytical system model, 18 of 19 poles are found with a total relative error of 0.05 (unitary weighting). This is the same order as would be suggested by examining the HSVs of the analytical system.

Fig. 9a and Fig. 9b show by visual examination that PC-CF clearly places the poles closer to the theoretical eigenvalues of the system than MF. Note that in this figure, the theoretical eigenvalues are marked with 'x's that are sized according to the square root of the HSV to give a visual indication of the important poles. Fig. 9c quantifies the accuracy of the pole location as described by (22), with unitary weighting on the poles, and with weighting according to the HSVs. In both cases, PC-CF is able to more accurately place the poles. The most important poles in this system (in this case, the 4 located closest to the imaginary axis) are found by both methods. This can be inferred from the decrease in error of MF from unitary weighting to HSV weighting, i.e. the error value of MF more closely matches that of PC-CF when using HSV weighting. A meaningful interpretation of this is that while both methods can find the most dominant poles, PC-CF can more accurately locate the less dominant poles.

While it is true in some cases that fitting using MF with a higher order and subsequently reducing to only the most important poles can result in similarly accurate pole locations, this is not necessarily true of systems such as this. Fig. 10 shows the results of using this method, which actually result in higher error. If the few poles closest to the origin (those with highest HSVs) are examined closely, it can be seen that MF places several poles in close proximity where before there was one. These "split" poles also share contributions to the system behavior, resulting in multiple "important" poles instead of one. This can be attributed to overfitting such that

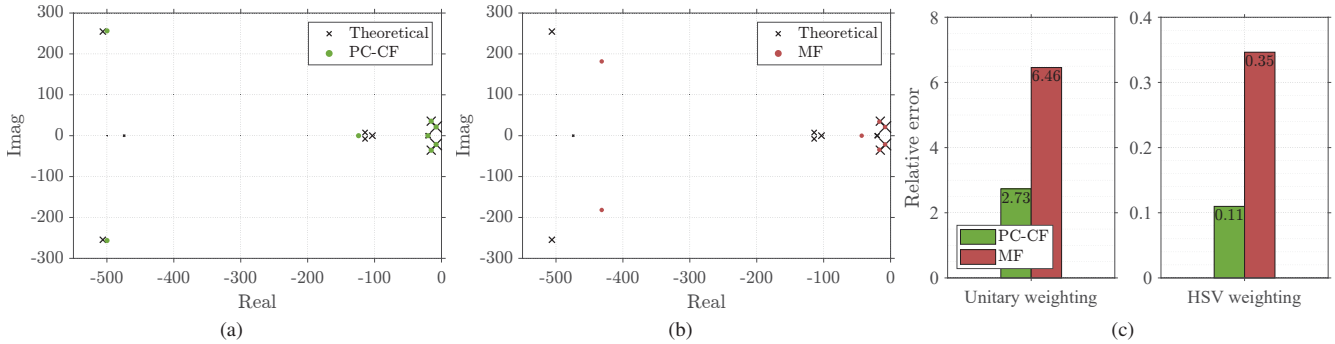

Fig. 9. Comparison of poles from fitting vs. example system eigenvalues. (a) Eigenvalues found by PC-CF. (b) Eigenvalues found by MF. (c) Eigenvalue accuracy comparison with unitary weighting on poles (UW) and weighting according to HSVs.

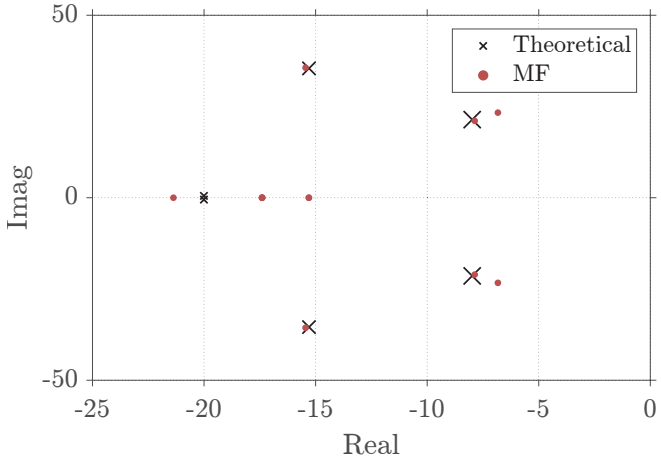

Fig. 10. Pole location using MF with high initial order (50) and reducing to 14 based on highest HSV poles, resulting in a unitary weighting error of 9.46 and HSV weighting error of 0.58.

small differences in the frequency response result in multiple nearby poles instead of one.

2) Frequency Response Fitting: The second measure of accuracy is the fitting of the frequency response data. Since this data is used to identify the system, a high degree of accuracy is expected. The sum of absolute errors (SAE) is used to find the total error, calculated as:

$$\text{SAE} = \sum_{j=1}^{J}\sum_{i=1}^{I}\sum_{f=1}^{F} ||H_0(j,i,f) - H(j,i,f)|| \qquad (24)$$

where H_0 is the reference data set for an output j, input i, and sample point at frequency f, and H is the fitted system at the same data point.

Table I shows the comparison of the accuracy for the frequency responses. According to the SAE in row 1 and 4, PC-CF without compaction performs better than MF (20.9 compared to 29.8). However, this is due to the change in weighting scheme from finding the poles and residues. This is discussed further in Section VI. Both methods of full compaction show increased error, as expected, although regardless of vector fitting methodology, full compaction based

TABLE I
FREQUENCY RESPONSE COMPARISON

Method	Sum of Absolute Errors	
	before refinement	after refinement
1. $PC-CF$	20.9	-
2. FC_{SVD}	335	59.0
3. FC_{HSV}	294	75.8
4. MF	29.8	-
5. FC_{SVD}	734	115
6. FC_{HSV}	296	107

on balanced truncation ($\mathbf{FC_{HSV}}$) (row 3 and 6) performs better than full compaction based on SVD (row 2 and 5).

The importance of improving the residue matrices after compaction can clearly be seen from this table, as the metrics are given before and after iterative refinement by `pem`. It is interesting to note that after improvement of the residue matrices, the two methods of compaction give far more similar accuracy. This indicates that, although $\mathbf{FC_{HSV}}$ is more accurate, the difference can largely be compensated for by refinement after compaction. Starting with PC-CF as a base for compaction results in reduction of error by approximately a factor of two compared to matrix fitting. However, the refinement process reduces the error by a factor of approximately 6. Therefore, iterative refinement is always recommended in the compaction process.

Fig. 11 shows an example of a frequency response comparison between the compacted and non-compacted systems. The compacted system after iterative refinement is used. Although there is increased error after compaction, the match is still highly accurate. This sample response is representative of the other input responses.

3) Effect of Compaction on Simulation Time: The result of compaction on simulation time for the resulting state-space models is examined. Ten seconds are simulated with a time step of 1×10^{-5}s using the Matlab function `lsim` for various levels of compaction to demonstrate the benefit of compacting the model. An arbitrary system with 60 poles, 10 inputs, and 6 outputs is used. Note that the Matlab function `sparss` is used to create sparse matrices for state-space

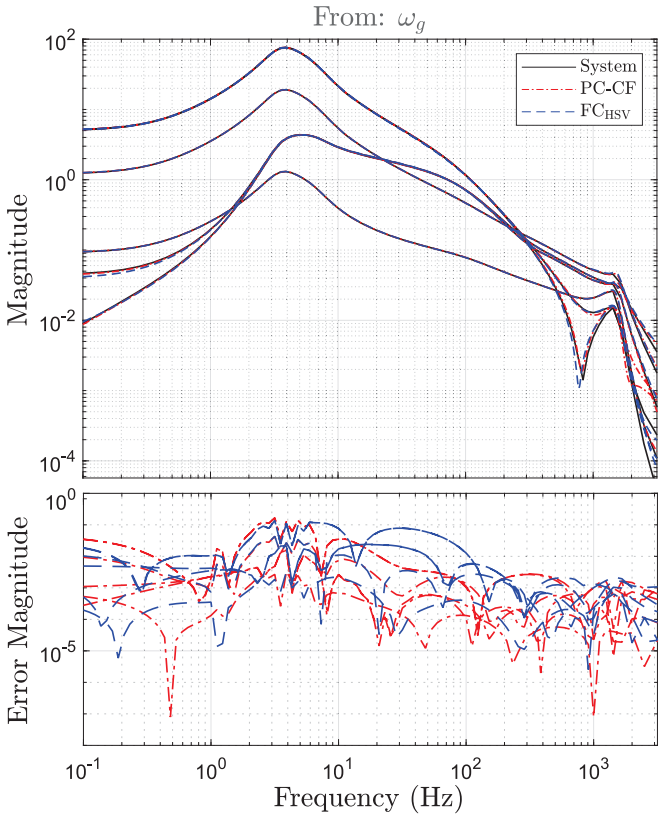

Fig. 11. Example of frequency response fitting for one input.

system. This takes advantage of the sparse nature of the non-compacted systems to give faster simulation times and a more fair comparison. It should be noted that the non-compacted system can be calculated according to [26] for additional computational savings; however, the fully compacted system is also simulated faster in this case without using `sparss`.

Fig. 12 shows the simulation time compared to the total order (including repeated poles). Full compaction (FC), with no repeated poles, leads to a simulation savings of 5.3 times, which aligns closely with the predicted savings, $I/2$, which, with 10 inputs, would predict a 5 times computational savings. Additionally, a minimal realization of this system which retains all information from the non-compacted system (called here minimal compaction (MC)), with a compaction threshold of zero, results in 44% faster computation time than no compaction (NC). This is for a system with 6 outputs and 10 inputs, so the minimal realization results in four repeating pole sets eliminated. For systems with a larger difference between number of outputs to inputs, the computational savings would be even further in the direction of full compaction. It should also be noted that minimal compaction results in no decrease in accuracy compared to no compaction. In cases of combining multiple state-space models, the simulation times will be compounded and reducing the times by even a factor of 2 will have significant impacts on the overall simulation time.

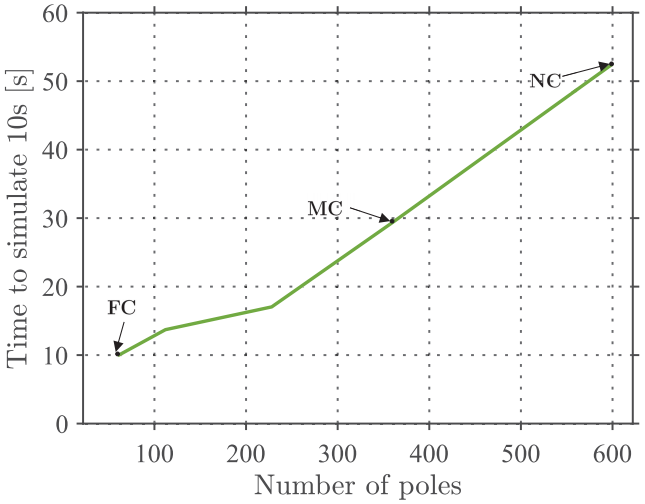

Fig. 12. Simulation times for no compaction (NC), minimal compaction (MC), and full compaction (FC), using 10^6 time steps.

VI. Discussion

This section summarizes some of the main findings and benefits of using the proposed methods, as well as discussion of their applicability.

A. Qualitative Advantages

There are several important results that can be taken from this work regarding vector fitting and compaction of MIMO systems:

- By applying the PC-CF method to a MIMO system, an appropriate order for the system can be obtained without knowledge of the system and without manually or iteratively selecting the order. This technique helps to prevent overfitting, while still using a sufficient order. This can be especially useful for systems with high levels of noise.
- PC-CF gives a model with improved eigenvalue-locating properties compared to matrix fitting. This can be useful in eigenvalue stability analyses, such as performed in [23], [27], [21].
- When a MIMO system is not square, i.e. there are an uneven number of outputs and inputs, the resulting vector-fitted state-space model can be compacted such that the poles are repeated only $\min(I, J)$ number of times. This can be done without loss in accuracy or information in the model.
- A vector-fitted MIMO state-space model can be compacted to reduce the number of repeated poles, although with an increased error. This error can be significantly reduced by optimizing the **B** and **C** matrices after compaction.
- Compaction using balanced reduction via Hankel singular values provides a more accurate initial compaction than the singular value decomposition method. A large portion of this difference can be compensated for, however, by refining the **B** and **C** matrices.

- Compaction of a model can greatly increase the computational efficiency of simulations, with greater efficiency associated with more compaction.

B. Qualitative Assessment

MF iteratively places the poles to minimize the error in frequency response while PC-CF has higher focus on correct pole location. However, in an eigenvalue analysis, the pole placement is of higher importance and MF can critically miscalculate the poles. In the first example, the poles found by MF are further to the left-hand side of the plane, implying a larger stability margin than actually exists.

In the fitting process, several weighting schemes can be applied to the frequency responses. For example, an inverse or inverse square root of the magnitude weighting can be applied so that low amplitude responses will be fitted with similar accuracy as the high amplitude frequencies. The most desirable weighting scheme will depend upon the application. When fully compacting a system, there are three distinct instances to apply a weighting scheme: pole location, residue fitting, and iterative refinement. Since the iterative refinement acts on the residue matrices **B** and **C**, the weighting scheme for iterative refinement should match that used for residue fitting. Note that only unitary weighting is readily possible with `pem`, and so other refinement tools or adaptations should be made if other weighting schemes are desired.

An inverse square root weighting was found to be the most suitable for pole location in both examples. However, after the poles are determined, a uniform weighting scheme is used for residue fitting and iterative refinement, which places greater importance on fitting high amplitude regions of the frequency response. This is because the resonance peaks are of highest concern in the second example. Note that since a different weighting scheme is used for pole placement and residue fitting, MF will not place the poles optimally to reduce the total error, giving a slightly higher error compared to PC-CF in Table I.

The time to find the poles using PC-CF is naturally increased as a high number of poles is used to fit to each input before collapsing. For the second example with an initial pole number of 50 per input and 30 iterations, PC-CF uses approximately 1.6 seconds to find the poles, as opposed to 0.3 seconds for MF. Of this 1.6 seconds, only 0.005 seconds are used to collapse the large initial pole set. Compaction using balanced reduction only implies a relatively small increase in computation time, taking approximately 0.05 seconds compared to 0.015 seconds using SVD. The CPU time of nonlinear iterative refinement, however, can incur a considerable computational effort. On the fully compacted model with a maximum of 30 iterations for 14 poles, `pem` uses approximately 5 seconds. This process does not scale well as the number of poles increases, taking 12 seconds with a 20 pole system. Therefore, a system with a high number of poles may have significantly increased calculation times if the compacted system is refined. The number of iterations also plays a direct role in computation time.

VII. Conclusion

This work has introduced a new method for applying vector fitting to system identification of MIMO systems, called pole-collapsing column fitting (PC-CF). It is shown that this method has improved common pole selection properties over matrix fitting for identifying the eigenvalues of the system, while still providing a common pole set capability. Additionally, this method does not need an order selection from the user and will automatically determine an appropriate order. This work has also demonstrated an improvement in methodology for compaction of the state-space systems to reduce the error introduced by compaction. PC-CF and the suggested compaction methodology are performed on an example system to demonstrate the effectiveness.

Further work can include refinement of the methodology for finding overlapping poles. As of now, a percentage tolerance in the real and imaginary axis is used; however, some improvement could likely be achieved by using more advanced clustering techniques, as well as by providing the option to specify a given number of poles to be found. It would be useful to investigate cases such as large systems where MF might have excessive computation times solving the least-squares problem, while PC-CF could solve it column by column. Additionally, it would be relevant to compare the performance of PC-CF to other system identification methods.

References

[1] K. Ogata, *Modern Control Engineering*, 5th ed. Pearson, Aug. 2009.

[2] P. S. Kundur and O. P. Malik, *Power System Stability and Control*, 2nd ed. McGraw-Hill Education, 2022. [Online]. Available: https://www.accessengineeringlibrary.com/content/book/9781260473544

[3] L. Ljung, *System identification: theory for the user*, 2nd ed., ser. Prentice Hall information and system sciences series. Upper Saddle River, NJ: Prentice Hall PTR, 1999.

[4] B. Gustavsen and A. Semlyen, "Rational approximation of frequency domain responses by vector fitting," *IEEE Transactions on Power Delivery*, vol. 14, no. 3, pp. 1052–1061, Jul. 1999. [Online]. Available: http://ieeexplore.ieee.org/document/772353/

[5] ——, "Simulation of transmission line transients using vector fitting and modal decomposition," *IEEE Transactions on Power Delivery*, vol. 13, no. 2, pp. 605–614, Apr. 1998.

[6] X. Hu, L. Chaudhari, S. Lin, S. Stanton, S. Asgari, and W. Lian, "A state space thermal model for HEV/EV battery using vector fitting," in *2012 IEEE Transportation Electrification Conference and Expo (ITEC)*. Dearborn, MI, USA: IEEE, Jun. 2012, pp. 1–8. [Online]. Available: https://ieeexplore.ieee.org/document/6243450

[7] W. Zhou, R. E. Torres-Olguin, F. Gothner, J. Beerten, M. K. Zadeh, Y. Wang, and Z. Chen, "A robust circuit and controller parameters' identification method of grid-connected voltage-source converters using vector fitting algorithm," *IEEE Journal of Emerging and Selected Topics in Power Electronics*, vol. 10, no. 3, pp. 2748–2763, Jun. 2022. [Online]. Available: https://ieeexplore.ieee.org/document/9354806/

[8] A. Arda Ozdemir and S. Gumussoy, "Transfer function estimation in system identification toolbox via vector fitting," *IFAC-PapersOnLine*, vol. 50, no. 1, pp. 6232–6237, Jul. 2017. [Online]. Available: https://linkinghub.elsevier.com/retrieve/pii/S2405896317315045

[9] B. Gustavsen, "Improving the pole relocating properties of vector fitting," *IEEE Transactions on Power Delivery*, vol. 21, no. 3, pp. 1587–1592, Jul. 2006. [Online]. Available: http://ieeexplore.ieee.org/document/1645204/

[10] D. Deschrijver, M. Mrozowski, T. Dhaene, and D. De Zutter, "Macromodeling of multiport systems using a fast implementation of the vector fitting method," *IEEE Microwave and Wireless Components Letters*, vol. 18, no. 6, pp. 383–385, Jun. 2008. [Online]. Available: http://ieeexplore.ieee.org/document/4530747/

[11] B. Gustavsen, "Computer code for rational approximation of frequency dependent admittance matrices," *IEEE Transactions on Power Delivery*, vol. 17, no. 4, pp. 1093–1098, Oct. 2002. [Online]. Available: http://ieeexplore.ieee.org/document/1046889/
[12] "Matrix Fitting Toolbox." [Online]. Available: https://www.sintef.no/projectweb/vectorfitting/downloads/matrix-fitting-toolbox/
[13] B. Gustavsen and A. Semlyen, "A robust approach for system identification in the frequency domain," *IEEE Transactions on Power Delivery*, vol. 19, no. 3, pp. 1167–1173, Jul. 2004. [Online]. Available: http://ieeexplore.ieee.org/document/1308342/
[14] S. Grivet-Talocia and B. Gustavsen, *Passive macromodeling*. Hoboken, New Jersey: John Wiley & Sons, Inc, 2016.
[15] P. Van Overschee and B. De Moor, "N4SID: Subspace algorithms for the identification of combined deterministic-stochastic systems," *Automatica*, vol. 30, no. 1, pp. 75–93, Jan. 1994. [Online]. Available: https://linkinghub.elsevier.com/retrieve/pii/0005109894902305
[16] H. Van Der Auweraer and B. Peeters, "Discriminating physical poles from mathematical poles in high order systems: use and automation of the stabilization diagram," in *Proceedings of the 21st IEEE Instrumentation and Measurement Technology Conference (IEEE Cat. No.04CH37510)*. Como, Italy: IEEE, 2004, pp. 2193–2198. [Online]. Available: http://ieeexplore.ieee.org/document/1351525/
[17] E. Reynders, J. Houbrechts, and G. De Roeck, "Fully automated (operational) modal analysis," *Mechanical Systems and Signal Processing*, vol. 29, pp. 228–250, May 2012. [Online]. Available: https://linkinghub.elsevier.com/retrieve/pii/S0888327012000088
[18] A. Varga, "Balancing free square-root algorithm for computing singular perturbation approximations," in *Proceedings of the 30th IEEE Conference on Decision and Control*, Dec. 1991, pp. 1062–1065 vol.2.
[19] S. D'Arco, J. A. Suul, and O. B. Fosso, "A virtual synchronous machine implementation for distributed control of power converters in SmartGrids," *Electric Power Systems Research*, vol. 122, pp. 180–197, May 2015. [Online]. Available: https://linkinghub.elsevier.com/retrieve/pii/S0378779615000024
[20] O. Mo, S. D'Arco, and J. A. Suul, "Evaluation of virtual synchronous machines with dynamic or quasi-stationary machine models," *IEEE Transactions on Industrial Electronics*, vol. 64, no. 7, pp. 5952–5962, Jul. 2017. [Online]. Available: http://ieeexplore.ieee.org/document/7781612/
[21] M. K. Bakhshizadeh, F. Blaabjerg, J. Hjerrild, L. Kocewiak, and C. L. Bak, "Improving the impedance-based stability criterion by using the vector fitting method," *IEEE Transactions on Energy Conversion*, vol. 33, no. 4, pp. 1739–1747, Dec. 2018. [Online]. Available: https://ieeexplore.ieee.org/document/8391731/
[22] L. Reis, A. M. Smith, S. D'Arco, and J. A. Suul, "Applying Vector Fitting for Measurement-based Multiple-Input Multiple-Output Model Identification of a Grid-Forming Converter," in *Powering solutions for decarbonized and resilient future smartgrids*, Grenoble, France, Oct. 2023. [Online]. Available: https://hdl.handle.net/11250/3115525
[23] A. Rygg, M. Amin, M. Molinas, and B. Gustavsen, "Apparent impedance analysis: A new method for power system stability analysis," in *2016 IEEE 17th Workshop on Control and Modeling for Power Electronics (COMPEL)*. Trondheim, Norway: IEEE, Jun. 2016, pp. 1–7. [Online]. Available: http://ieeexplore.ieee.org/document/7556667/
[24] W. Zhou, Y. Wang, and Z. Chen, "Reduced-Order Modelling Method of Grid-Connected Inverter with Long Transmission Cable," in *IECON 2018 - 44th Annual Conference of the IEEE Industrial Electronics Society*. D.C., USA: IEEE, Oct. 2018, pp. 4383–4389. [Online]. Available: https://ieeexplore.ieee.org/document/8591133/
[25] C. Sun and J. Hahn, "Parameter reduction for stable dynamical systems based on Hankel singular values and sensitivity analysis," *Chemical Engineering Science*, vol. 61, no. 16, pp. 5393–5403, Aug. 2006. [Online]. Available: https://linkinghub.elsevier.com/retrieve/pii/S0009250906002557
[26] B. Gustavsen and H. M. J. De Silva, "Inclusion of Rational Models in an Electromagnetic Transients Program: Y-Parameters, Z-Parameters, S-Parameters, Transfer Functions," *IEEE Transactions on Power Delivery*, vol. 28, no. 2, pp. 1164–1174, Apr. 2013. [Online]. Available: http://ieeexplore.ieee.org/document/6480900/
[27] M. K. Bakhshizadeh, C. Yoon, J. Hjerrild, C. L. Bak, L. H. Kocewiak, F. Blaabjerg, and B. Hesselbaek, "The application of vector fitting to eigenvalue-based harmonic stability analysis," *IEEE Journal of Emerging and Selected Topics in Power Electronics*, vol. 5, no. 4, pp. 1487–1498, Dec. 2017. [Online]. Available: http://ieeexplore.ieee.org/document/7982617/

Andrew Macmillan Smith (M'2023) received a BSc in Mechanical Engineering from the University of California, Santa Barbara (UCSB) in 2016 and then a joint MSc in Renewable Energy in the Marine Environment in 2022, with a specialization in "Power Electronics and Control for Offshore Renewable Energy Systems" from the University of Strathclyde (UoS), University of the Basque Country (UPV/EHU), and the Norwegian University of Science and Technology (NTNU). He now works at Sintef Energy Research in Trondheim, Norway.

Salvatore D'Arco received the M.Sc. and Ph.D. degrees in electrical engineering from the University of Naples "Federico II," Naples, Italy, in 2002 and 2005, respectively. From 2006 to 2007, he was a postdoctoral researcher at the University of South Carolina, Columbia, SC, USA. In 2008, he joined ASML, Veldhoven, the Netherlands, as a Power Electronics Designer consultant, where he worked until 2010. From 2010 to 2012, he was a postdoctoral researcher in the Department of Electric Power Engineering at the Norwegian University of Science and Technology (NTNU), Trondheim, Norway. In 2012, he joined SINTEF Energy Research where he currently works as a Chief Research Scientist. He is the author of more than 130 scientific papers and is the holder of one patent. His main research activities are related to control and analysis of power-electronic conversion systems for power system applications, including real-time simulation and rapid prototyping of converter control systems.

Jon Are Suul (M'11) received the MSc. degree in energy and environmental engineering and the PhD degree in electric power engineering from the Norwegian University of Science and Technology (NTNU), Trondheim, Norway, in 2006 and 2012, respectively.

From 2006 to 2007, he was with SINTEF Energy Research, Trondheim, where he was working with simulation of power electronic converters and marine propulsion systems until starting his Ph.D. studies. Since 2012, he has been a Research Scientist with SINTEF Energy Research, first in a part-time position while working as a part-time Postdoctoral Researcher with the Department of Electric Power Engineering of NTNU until 2016. Since August 2017, he is also an Adjunct Associate Professor with the Department of Engineering Cybernetics, NTNU. His research interests are mainly related to modeling, analysis, and control of power electronic converters in power systems, renewable energy applications, and electrification of transport.

Dr. Suul is an Editor of the IEEE JOURNAL OF EMERGING AND SELECTED TOPICS IN POWER ELECTRONICS. He is also an Associate Editor for the IEEE TRANSACTIONS ON ENERGY CONVERSION and the IEEE JOURNAL OF EMERGING AND SELECTED TOPICS IN INDUSTRIAL ELECTRONICS.

Bjørn Gustavsen (M'94–SM'2003–F'2014) was born in Norway in 1965. He received the M.Sc. degree and the Dr. Ing. degree in Electrical Engineering from the Norwegian Institute of Technology in Trondheim, Norway, in 1989 and 1993, respectively. Since 1994 he has been working at SINTEF Energy Research, currently as Chief Research Scientist. His interests include simulation of electromagnetic transients and modeling of frequency dependent effects. He spent 1996 as a Visiting Researcher at the University of Toronto, Canada, and the summer of 1998 at the Manitoba HVDC Research Centre, Winnipeg, Canada. He was Marie Curie Fellow at the University of Stuttgart, Germany, August 2001–August 2002.